American Journal of Biochemistry and Biotechnology

Original Research Paper

Sonoporation Enhances Liposome Mediated EcTRAF4 siRNA Delivery in SaB-1 Cells

Meng Han Chen and Wang Chung Ping

Institute of Veterinary Medicine, National Taiwan University, Taipei, Taiwan

Article history
Received: 26-03-2023
Revised: 28-04-2023
Accepted: 03-05-2023

Corresponding Author:
Meng Han Chen
Institute of Veterinary Medicine, National Taiwan University, Taipei, Taiwan
Email: eric122821@gmail.com

Abstract: Sonoporation, which is the perforation of cell membranes using ultrasound and microbubble, has been shown to facilitate the liposome-mediated delivery of nucleotides in mammalian cells. The effect has not yet been tested in non-vertebrate species such as fish. Since adenoviral vector delivery is associated with tumorigenicity and electroporation is affected by the ions content in culture water, sonoporation may be an ideal means of enhancing the transfection efficiency in aquaculture. Hence, in this study, sonoporation was used to enhance the transfection efficiency of siEcTRAF4 lipoplexes, which inhibits Viral Haemorrhagic Septicaemia Virus (VHSV) infection, in SaB-1 cells. However, the effect of sonoporation parameters on transfection efficiency must be elucidated, so the effect of acoustical pressures and bubble-to-cell distance on membrane permeabilization of SaB-1 cells was analyzed. Sonoporation was found to assist the delivery of siEcTRAF4 lipoplexes into SaB-1 cells and to reduce viral replication after the VHSV challenge. These results imply that a prognostic technique against VHSV infection that combines sonoporation and siEcTRAF4 lipoplexes may be applicable in aquaculture in the future.

Keywords: Microbubbles, Cavitation, Sonoporation, UCA, Ultrasound, Cytoskeleton

Introduction

EcTRAF4, which is Tumor necrosis factor Receptor Associated Factors4 (TRAF4) homolog of the gilthead seabream, has been shown to inhibit pro-inflammatory cytokines production after VHSV infection. EcTRAF4 siRNA is regarded as a potential therapeutic agent for treating Viral hemorrhagic Septicaemia Virus (VHSV) that is infected with VHSV and would otherwise suffer mass mortality (Wu *et al*., 2021). Due to its susceptibility to nuclease degradation, siRNA is often delivered with liposome encapsulation, which together, is called a lipoplexe. However, the low transfection efficiency rate of lipoplexes in fish cells has hampered its application in aquaculture (Izadifar *et al*., 2017). Hence, sonoporation techniques are tested to determine their capacity to improve the transfection efficiency of siRNA lipoplexes in fish cells in this study.

Sonoporation, using low-frequency ultrasound irradiation to transient perforate the cell membrane and allow the uptake of nucleotide or drug in the adjacent cavitation bubbles, has recently drawn great attention (Lentacker *et al*., 2014; Miller *et al*., 2002; Van Wamel *et al*., 2006). This potential technique for gene therapy has been investigated for a wide range of mammalian systems (Tomizawa *et al*., 2013), while few non-vertebrate species such as fish have been tested. This study uses the sonoporation technique in the delivery of therapeutic siRNA in SaB-1 with the goal of making the technique applicable to aquaculture in the future.

To provide a comprehensive understanding of the effect of sonoporation on SaB-1 cells, sonoporation-induced cellular responses such as membrane permeabilization and cytoskeleton disassembly generated under various acoustic driving pressure and microbubble cell distances were analyzed. A previous study has shown that non-acoustic parameters, such as microbubble cell distances are strongly correlated with the degree of sonoporation (Qin *et al*., 2016). Some studies have reported that sonoporation efficiency increases as bubble cell distance decreases (Miller *et al*., 2002; Qin *et al*., 2016; Yang *et al*., 2020).

The signal of cavitation activity was recorded using a passively coupled ultrasound transducer and quantified as Inertial Cavitation Dose (ICD) (Chen *et al*., 2003). Linearly positive correlations between acoustic driving pressure, ICD, sonoporation pore size, and transfection efficiency in MCF-7 cells were reported (Qiu *et al*., 2010) indicating that

sonoporation activity was responsible for the change in transfection efficiency.

Propidium Iodide (PI) is normally excluded by the cell membrane, but damage to the membrane by sonoporation allows PI to permeate the sonoporated cells and bind to nucleotides in the cytoplasm and nuclei, hence PI was used as a sonoporation tracer to quantitatively measure the extent of membrane permeabilization. On the other hand, a Green Fluorescence Protein (GFP) α-tubulin fusion protein was used to monitor the extent of cytoskeleton disassembly that was induced by sonoporation. The enhancement of red fluorescence would represent the increasing PI uptake through sonoporated membrane pores, while the decay of green fluorescence represents sonoporation-induced cytoskeleton disassembly.

Materials and Methods

Cell Culture

The SaB-1 cell line, derived from the fin tissue of gilthead seabream was grown in Dulbecco's Modified Eagle's Medium (DMEM) (Carlsbad, CA, USA) that was supplemented with 5% (w/w) Fetal Bovine Serum (FBS) (Sigma-Aldrich, St. Louis, MO, USA) and antibiotics (1 mg/mL penicillin and 100 u/mL streptomycin) (GIBCO®EU 10270) at 27°C in a humidified CO_2 incubator. The cells were labeled by a GFP α-tubulin fusion protein in order to measure the extent of cytoskeleton disassembly induced by sonoporation.

Microbubbles

Commercial microbubbles (UCA; TRUST Bio Sonics, Taiwan) with an average diameter of 1.5 µm were used as the cavitation agent in this study. Each bubble was comprised of a gas nucleus that was encapsulated by a phospholipid shell for acoustic pressure to trigger the sonoporation process. Microbubbles were added to the cell suspension 5 min before the ultrasound exposure at a cell-to-bubble ratio of 1:1 which was empirically found to give a balance between the sonoporation (>30%) effect and minimization of instant cell death (Chen *et al*., 2013).

Sonoporation Tracer

Propidium Iodide (PI; P4170, Sigma-Aldrich, St. Louis, MO, USA, excitation/emission maxima: 551/670 nm) was used as a fluorescence marker to measure the extent of membrane permeabilization. PI is excluded from the cell membrane normally, but as the membrane was damaged by sonoporation, PI can permeate the sonoporated cells and binds to nucleotides in the cytoplasm and nucleus (Haberl *et al*., 2013). PI was added to the OptiCell™ sample holder (0.25 µg/mL) and incubated for 5 min before adding the microbubbles.

Experimental System

The ultrasound exposure apparatus is comprised of an arbitrary waveform generator (33250 A, Agilent, Palo Alto, CA, USA), a broadband amplifier (2200 L, Electronics Innovation, Rochester, NY, USA), and a single-element focused piston transducer (1 MHz center frequency, A314S, Olympus Panametrics-NDT, Waltham, MA, USA). A 20 µs long pulse was applied. The irradiation time was 30 sec and the sound intensity was 1.5 W/cm^2. The in situ acoustic peak negative pressure at the focus was calibrated to be 0.1, 0.3, and 0.5 MPa, by using the NTR needle hydrophone (TNU001A, NTR Systems Inc., Seattle, WA, USA). The cells were grown on the upper wall of an OptiCell™ chamber. Ultrasound energy delivered by the ultrasound exposure apparatus would pass through a cylindrical polyacrylamide gel to focus on the SaB-1 cells. A fluorescence microscope (BX53, Olympus, Shinjuku, Tokyo, Japan) was used to monitor the morphology of the cell.

Cavitation Signal Analysis

Passive Cavitation Detection (PCD) system was used to measure the ultrasound-induced microbubble acoustic emission signals. The estimated Inertial Cavitation Dose (ICD) provides the amount of IC energy that was delivered over a certain ultrasound exposure duration under different treatment conditions. The acoustic signals that were scattered from the exposed suspension were received by the 5 MHz PCD transducer and digitized by the oscilloscope with a sampling frequency of 25 MHz. Each waveform of all sampled time series signals was first transformed to the frequency domain using Fast Fourier Transform (FFT). The amount of IC-induced broad-band noise was calculated as the Root Mean Square (RMS) amplitude of the FFT spectrum within a specific frequency window. Then these FFT and RMS amplitudes were plotted for all sampled waveforms as a function of exposure time. The cumulated ICD was defined as the area under this curve over the entire exposure.

MTT Assay

MTT assay was used to measure the cell viability of SaB-1 cells after sonoporation. The SaB-1 cells were seeded into a 96-well plate after the sonoporation experiment. On the following day, the culture medium was replaced with 80 µL of fresh medium and 20 µL (50 µg) of MTT solution at 10 mg/mL and incubated for an additional 2 h. After that, the formazan crystals were dissolved in 100 µL of dimethylsulfoxide. The

DOI: 10.3844/ajbbsp.2023.152.158

absorbance was measured at 570 nm using a microplate reader (Molecular Devices, Sunnyvale, CA, USA).

Colony Formation Efficiency Assay

A colony formation efficiency assay was used to determine the SaB-1 cell proliferation ability after sonoporation. After incubation, cells were loaded into 4.1 cm 2 tissue culture dishes (TPP, Switzerland) containing 1.5 mL of growth medium and then allowed to grow for 5 days. After that, the cells were fixed in 1 mL of 95% ETOH for 5 min and then stained with crystal violet solution (Sigma Aldrich, St. Louis, MO, USA). The number of cell colonies was observed using a light microscope (MBS 9, LOMO, St. Petersburg, Russia) the values were normalized to the control (no treatment).

Statistical Analysis

The data are presented as the mean ± standard error of the mean of at least six experimental replicates. Student's t-test was used to compare pairs of groups. All data were expressed as mean ± Standard Deviation (SD). Correlation analysis was defined according to the correlation determination coefficient (R^2). Data analysis was performed using SPSS version 17. (Origin lab Co, Northampton, MA, USA) software.

Results

Cytotoxicity and Proliferation of SaB-1 Cells after Sonoporation

The cytotoxicity and proliferation ability of SaB-1 cells was measured using the MTT test and colony formation efficiency test. The results showed that neither Sonoporation (SP) with acoustic pressure p of 5 Mpa and a bubble-to-cell distance d of 1.5 μm (p = 5 mPa, d = 1.5 μm) nor Lipofectamine 3000 treatments induced cytotoxicity in SaB-1 cells (Fig. 1A). However, in the SP (p = 5 mPa, d = 1.5 μm) and SP (p = 5 mPa, d = 1.5 μm) assisted Lipofectamine-siRNA lipoplexes delivery groups, GF-1 cell proliferation was reduced (Fig. 1B).

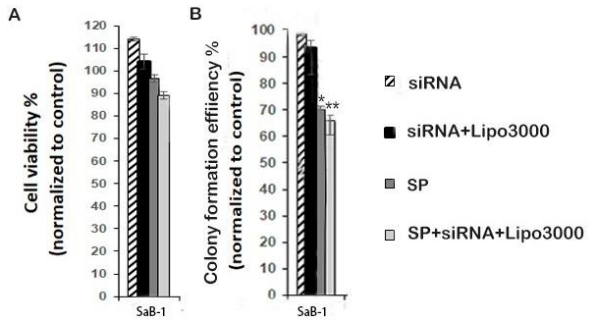

Fig. 1: Cytotoxicity and proliferation of SaB-1 cells after sonoporation

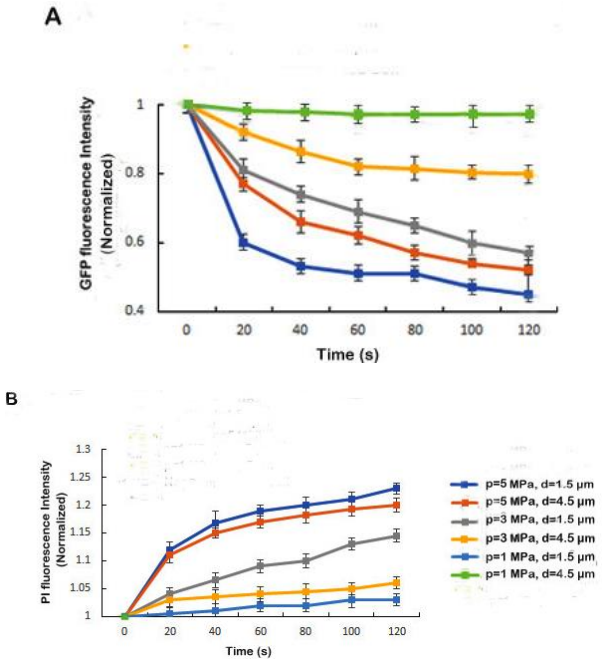

Fig. 2: Kinetics of cellular responses induced by sonoporation at various acoustic driving pressure and bubble cell distances

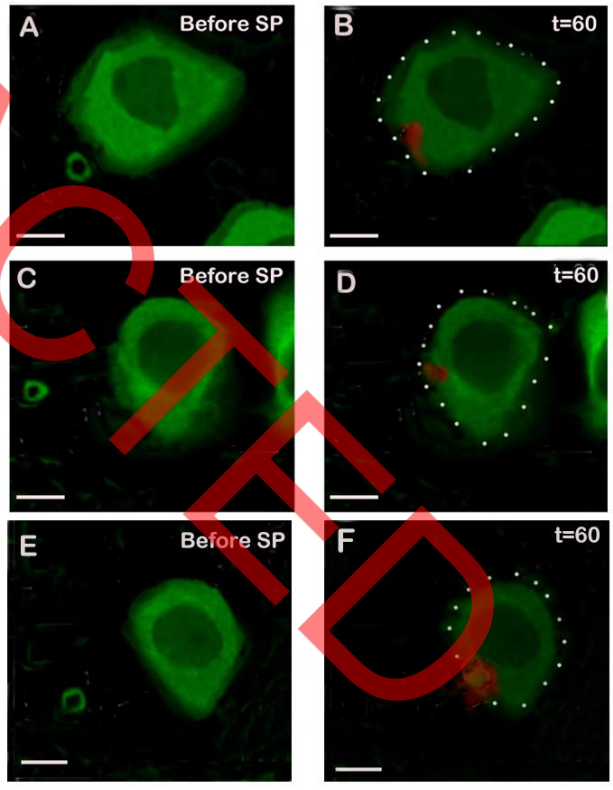

Fig. 3: Cell membrane permeabilization (PI, red fluorescence) and cytoskeleton disassembly (GFP, green fluorescence) at various acoustic driving pressure and microbubble cell distances

Kinetic of cellular responses induced by sonoporation at various acoustic driving pressure and bubble-cell distances Sonoporation (SP) with an acoustic pressure (p) of 5 Mpa and bubble-to-cell distance (d) of 1.5 µm (p = 5 MPa, d = 1.5 µm) most reduced the GFP fluorescence intensity (Fig. 2A) and most increased the PI fluorescence intensity (Fig. 2B) of SaB-1 cells. The SaB-1 cells in the SP (p = 1 MPa, d = 4.5 µm) group exhibited the least reduced GFP fluorescence intensity (Fig. 2A) and the least increased PI fluorescence intensity (Fig. 2B).

Cell membrane permeabilization (PI, red fluorescence) and cytoskeleton disassembly (GFP, green fluorescence) at varied acoustic driving pressure and microbubble cell distances confocal microscope were used to obtain the fluorescence images of membrane permeabilization (red fluorescence) and cytoskeleton disassembly (GFP, green fluorescence) induced by sonoporation. Various acoustic driving pressures (p) and bubble cell distance (d) were tested. The result showed that Sonoporation (SP) with acoustic pressure (p) of 3 Mpa and bubble-to-cell distance (d) of 1.5 µm (p = 3 MPa, d = 1.5 µm) had more PI fluorescence (red) increase (Fig. 3A-B) than the SP (p = 3 MPa, d = 4.5 µm) group (Fig. 3C-D). In addition, SP (p = 5 MPa, d = 4.5 µm) group (E, F) had more PI fluorescence (red) increase than the SP (p = 3 MPa, d = 4.5 µm) group (C, D).

EcTRAF4 mRNA Level after Sonoporation-Assisted Lipo3000-SiEcTRAF4 Lipoplexes Delivery

The EcTRAF4 mRNA level after sonoporation-assisted Lipofectamine 3000-EcTRAF4 siRNA lipoplexes (Lipo3000-siEcTRAF4) delivery was measured using real-time PCR (RTq-PCR). Table 1 presents the primers that were used. Lipo3000-siEcTRAF4 silencing with sonoporation (SP) with parameters p = 5 MPa, d = 1.5 µm; p = 5 MPa, d = 4.5 µm or p = 3 MPa, d = 1.5 µm were more significant compared with siCTRL, EcTRAF4 siRNA and Lipo 3000-siEcTRAF4 silencing. However, Lipo 3000-siEcTRAF4 silencing assisted by SP with parameters p = 3 MPa, d = 4.5 µm, p = 1 MPa, d = 4.5 µm or p = 1 MPa, d = 1.5 µm did not (Fig. 4).

Effect of Sonoporation-Assisted Delivery of SiEcTRAF4 Lipoplexes on Virus Replication in SaB-1 Cells after VHSV Infection

The effects of Sonoporation (SP) (p = 5 MPa, d = 1.5 µm) assisted delivery of siEcTRAF4 lipoplexes on CP (A) and RdRp (B) mRNA expression in SaB-1 cells after VHSV infection were obtained using RT-qPCR. In the group with the SP (p = 5 MPa, d = 1.5 µm) assisted delivery of siEcTRAF4 lipoplexes, the decreases in CP (Fig. 5A) and RdRp (Fig. 5B) were greater than in the group without SP assistance.

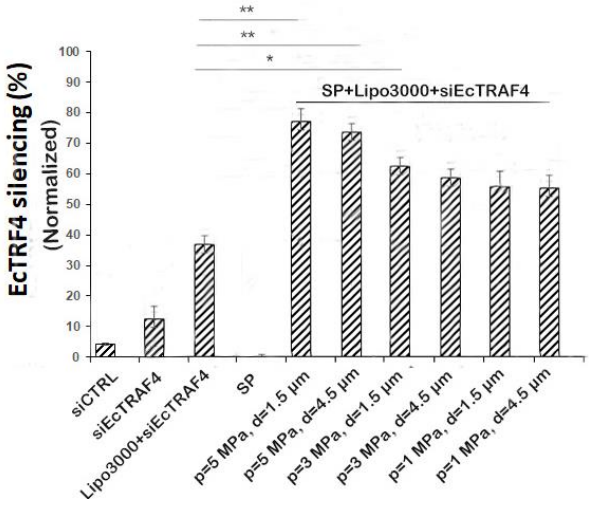

Fig. 4: EcTRAF4 mRNA level after sonoporation

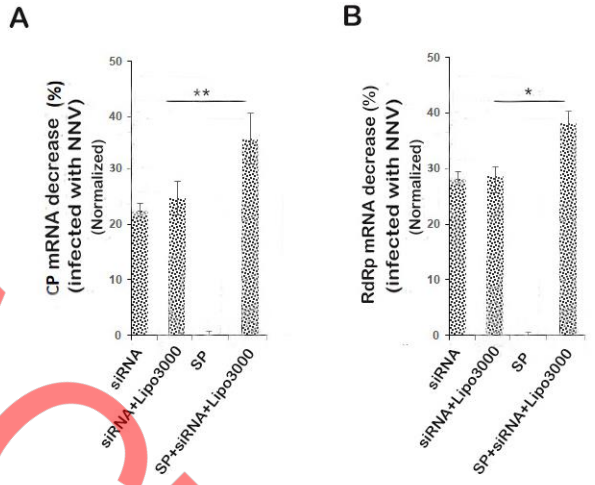

Fig. 5: Effect of sonoporation-assisted siEcTRAF4 lipoplexes delivering on VHSV replication

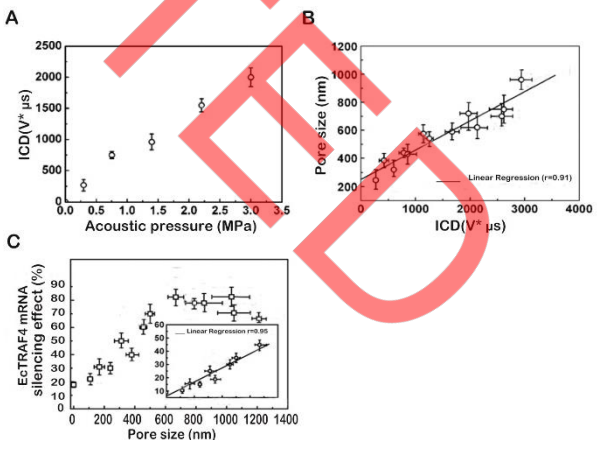

Fig. 6: Pairwise correlations between acoustic pressure, ICD, pore size, and EcTRAF4 mRNA silencing effect after sonoporation

Table 1: RT-qPCR primers used in this study

RT-qPCR Primers	Sequence
EcTRAF4 forward	5'CTACTATTGATCAACGGTGAACA3'
EcTRAF4 reverse	5'CCAGTCCACGCTAGTCGTACTCT3'
CP(VHSV) forward	5'CTACAGACAACGATCACACCTTC3'
CP(VHSV) reverse	5'CAATCAGCAACACTGCTGCGACA3'
RdRp forward	5'GTCTCCCGTGAGGTTAAGGATG3'
RdRp reverse	5'CTTGAATAGACAACGGTGAACA3'
β-actin forward	5'CCAGACAGACGGTGGCAACTC3'
β-actin reverse	5'CCCATCAATGTCACGCACGTAT3'

Capsid Protein (CP)

Pairwise Correlations Between Acoustic Pressure, ICD, Pore Size, and EcTRAF4 mRNA Silencing Effect after Sonoporation

The result showed that the correlations between acoustic pressure and Inertial Cavitation Dosage (ICD) (Fig. 6A), ICD, and pore size (Fig. 6B) were positive. However, the EcTRAF4 silencing effect increased only with the raised pore size in the initial stage (smaller than 630 nm), after which it was saturated (Fig. 6C).

Discussion

Sonoporation by microbubble-mediated ultrasound exposure has been shown to be a promising technique for the delivery of drugs and genes in many mammals (Escoffre *et al*., 2013; Ter Haar, 2007). However, knowledge concerning sonoporation in invertebrates, such as fish, is lacking. Hence, in this study, sonoporation was used to facilitate the delivery of Lipofectamine carried EcTRAF4 siRNA (EcTRAF4 siRNA lipoplexe) to SaB-1. In the result of confocal microscope images, the increase of red fluorescence from the post-sonoporated cells compared with the pre-sonoporated cells represents the increasing PI uptake through sonoporated membrane pores, while the decay of green fluorescence represents sonoporation induced cytoskeleton disassembly (Fig. 3). The evolutions of PI uptake and α-tubulin cytoskeleton disruption over time were well fitted, validating the correlation between these two concurrent activities (Fig. 2). Additionally, the three positives pairwise correlations between acoustic pressure, Inertial Cavitation Dosage (ICD) (signal of cavitation activity), pore size and silencing effect (Fig. 6) reveals that the increased EcTRAF4 silencing effect was induced by sonoporation.

Acoustic pressure is considered a critical determinant factor for nucleotide or drug uptake through sonoporation (De Cock *et al*., 2015). As a result, increased acoustic pressure and reduced bubble-to-cell distance induced more significant membrane permeabilization (Fig. 2A- 3), cytoskeleton disassembly (Fig. 2B-3), and EcTRAF4 mRNA silencing effect (Fig. 5). An acoustic pressure above 5 MPa induced a PI intensity that was extremely similar to that at 5 MPa (data not shown) and an acoustic pressure of 5 Mpa did not induced significant cytotoxicity (Fig. 1A), implying that the optimal acoustic pressure for the sonoporation of SaB-1 cell may be 5 MPa: A higher pressure may result in cellular damage without enhancing siRNA transfection efficiency. This finding is consistent with a previous report that transfection efficiency increased only with the raised acoustic pressure and ICD at the initial stage and then tended to saturate due to the formation of extra-large membrane pores induced by the delivery of excessive energy (Yang *et al*., 2020). Excessive acoustic energy either causes the contraction of the cell nucleus (Hu *et al*., 2014), disrupts downstream cellular hemostasis (Duan *et al*., 2021), or results in irreversible large membrane pore formation (Leow *et al*., 2015) and the subsequent cell death (Zhong *et al*., 2011).

A previous study has demonstrated that Inertial Cavitation (IC) activities that accumulate during sonoporation can be quantified as IC Dose (ICD) based on Passive Cavitation Detection (PCD) method (Lai *et al*., 2006). The assessment of the sonoporation-mediated siRNA silencing effect could thus be correlated with ICD measurements and this finding is consistent with our result (Fig. 6).

Other factors that affect sonoporation-mediated transfection are the microbubble concentration (Qiu *et al*., 2010), numerical bubble-to-cell ratio (Fan *et al*., 2014) (Guzmán *et al*., 2003), and the variation in cell morphologies with locations of the microbubbles (lamellipodia or cell body) relative to the cells (Ross *et al*., 2002). These factors still must be evaluated in the future before the *in vivo* stage.

With respect to the therapeutic application of sonoporation in aquaculture. UCAs are extremely sensitive to ultrasound exposure and is critical to localize UCAs within certain mucosal tissue areas to prevent adverse organ damage or side effects and to minimize the required sound pressure. Newly developed targeting agents, yet to be approved, can increase binding efficacy to target tissue areas and also decrease the required sound pressure (Izadifar *et al*., 2017), greatly favoring use in aquaculture.

The (A) cytotoxicity and (B) colony-forming efficiency of SaB-1 cells that were treated with EcTRAF4 siRNA, Lipofectamine 3000-encapsulated EcTRAF4 siRNA, Sonoporation (SP) (p = 5 MPa, d =1.5 μm) and

Sonoporation (SP) + Lipofectamine 3000 encapsulated EcTRAF4 siRNA, were measured. Results are presented as means ± SDs of at least three different measurements per sample and were normalized to control p; acoustic driving pressure, d; bubble to cell distance.

The kinetics of (A) cytoskeleton disassembly (GFP fluorescence) and (B) membrane permeabilization (PI fluorescence) that were induced by sonoporation at different acoustic driving pressures (p) and bubble to cell distance (d) over a 120 s period were measured. The number of sonoporated cells observed under individual pressures is n = 10.

Fluorescence images of membrane permeabilization (red fluorescence) and cytoskeleton disassembly (GFP, green fluorescence) that were induced by sonoporation at different acoustic driving pressures (p) and bubble cell distance (d), (A, B) p = 3 MPa, d = 1.5 μm; (C, D) p = 3 MPa, d = 4.5 μm; (E, F) p = 5 MPa, d = 4.5 μm, were obtained using confocal microscope. The boundaries of each cell are shown as dot lines and the scale bar represents 10 μm.

The mRNA expression levels of EcTRAF4 after control siRNA (siCTRL), EcTRAF4 siRNA, Lipofectamine 3000 encapsulated EcTRAF4 siRNA, Sonoporation (SP) and Sonoporation (SP) + Lipofectamine 3000 encapsulated EcTRAF4 siRNA treatment at different acoustic driving pressures (p) and bubble to cell distance (d) were measured. The silencing percentages were calculated from relative mRNA expression values normalized to untreated control. Values are represented as the mean ± S.D. (n = 3).

The effects of Sonoporation (SP) (p = 5 MPa, d = 1.5 μm) assisted siEcTRAF4 lipoplexes delivering on CP (A) and RdRp (B) mRNA expression in SaB-1 cells after VHSV infection were obtained using RT-qPCR. Values are represented as the mean ± S.D. (n = 3). The percentages were calculated from relative mRNA and normalized to untreated control.

The correlations between (A) acoustic pressure and ICD, (B) ICD and pore size (C) pore size and EcTRAF4 mRNA silencing effect after sonoporation (p = 3 MPa, d = 1.5 μm) were evaluated.

Conclusion

This study showed that sonoporation enhances liposome-mediated EcTRAF4 siRNA delivery in SaB-1 cells. The effect of sonoporation parameters including acoustic pressure and bubble cell distances on cellular response were provided. The results showed that a more significant cell membrane deformation could be achieved by increasing the acoustic pressure or reducing the bubble cell distance. The strong pairwise correlations between acoustic pressure, Inertial Cavitation Dosage (ICD), pore size, and silencing effect reveals that the increased EcTRAF4 silencing effect was induced by sonoporation. Taken together, these results reveal that sonoporation can facilitate liposome-mediated siRNA delivery and can decrease the VHSV replication number in fish cells following the VHSV challenge. A prognostic technique against VHSVV infection that combines sonoporation and EcTRAF4 siRNA may be applicable in aquaculture in the future.

Acknowledgment

We acknowledge all the staff members of the Institute of biochemistry for their cooperation to conduct this research.

Funding Information

The authors have not received any financial support or funding to report.

Author's Contributions

Chen Meng Han: All the experiment process and designed.

Wang Chung Ping: Article written.

Availability of Data and Materials

The datasets during and analysed during the current study available from the corresponding author on reasonable request.

Ethics

This article is original and contains unpublished material. The corresponding author confirms that all of the other authors have read and approved the manuscript and no ethical issues involved.

References

Chen, W. S., Brayman, A. A., Matula, T. J., & Crum, L. A. (2003). Inertial cavitation dose and hemolysis produced *in vitro* with or without Optison®. *Ultrasound in Medicine & Biology*, *29*(5), 725-737. https://doi.org/10.1016/S0301-5629(03)00013-9

Chen, X., Wan, J. M., & Alfred, C. H. (2013). Sonoporation as cellular stress: Induction of morphological repression and developmental delays. *Ultrasound in Medicine & Biology*, *39*(6), 1075-1086. https://doi.org/10.1016/j.ultrasmedbio.2013.01.008

De Cock, I., Zagato, E., Braeckmans, K., Luan, Y., de Jong, N., De Smedt, S. C., & Lentacker, I. (2015). Ultrasound and microbubble mediated drug delivery: Acoustic pressure as determinant for uptake via membrane pores or endocytosis. *Journal of Controlled Release*, *197*, 20-28. https://doi.org/10.1016/j.jconrel.2014.10.031

Duan, X., Zhou, Q., Wan, J. M., & Yu, A. C. (2021). Sonoporation generates downstream cellular impact after membrane resealing. *Scientific Reports*, *11*(1), 5161. https://doi.org/10.1038/s41598-021-84341-3

Escoffre, J. M., Zeghimi, A., Novell, A., & Bouakaz, A. (2013). *In-vivo* gene delivery by sonoporation: Recent progress and prospects. *Current Gene Therapy*, *13*(1), 2-14. https://doi.org/10.2174/1566523211313010002

Fan, Z., Chen, D., & Deng, C. X. (2014). Characterization of the dynamic activities of a population of microbubbles driven by pulsed ultrasound exposure in sonoporation. *Ultrasound in Medicine & Biology*, *40*(6), 1260-1272. https://doi.org/10.1016/j.ultrasmedbio.2013.12.002

Guzmán, H. R., McNamara, A. J., Nguyen, D. X., & Prausnitz, M. R. (2003). Bioeffects caused by changes in acoustic cavitation bubble density and cell concentration: A unified explanation based on cell-to-bubble ratio and blast radius. *Ultrasound in Medicine & Biology*, *29*(8), 1211-1222. https://doi.org/10.1016/S0301-5629(03)00899-8

Haberl, S., Kandušer, M., Flisar, K., Hodžić, D., Bregar, V. B., Miklavčič, D., ... & Pavlin, M. (2013). Effect of different parameters used for *in vitro* gene electrotransfer on gene expression efficiency, cell viability and visualization of plasmid DNA at the membrane level. *The Journal of Gene Medicine*, *15*(5), 169-181. https://doi.org/10.1002/jgm.2706

Hu, Y., Wan, J. M., & Alfred, C. H. (2014). Cytomechanical perturbations during low intensity ultrasound pulsing. *Ultrasound in Medicine & Biology*, *40*(7), 1587-1598. https://doi.org/10.1016/j.ultrasmedbio.2014.01.003

Izadifar, Z., Babyn, P., & Chapman, D. (2017). Mechanical and biological effects of ultrasound: A review of present knowledge. *Ultrasound in Medicine & Biology*, *43*(6), 1085-1104. https://doi.org/10.1016/j.ultrasmedbio.2017.01.023

Lai, C. Y., Wu, C. H., Chen, C. C., & Li, P. C. (2006). Quantitative relations of acoustic inertial cavitation with sonoporation and cell viability. *Ultrasound in Medicine & Biology*, *32*(12), 1931-1941. https://doi.org/10.1016/j.ultrasmedbio.2006.06.020

Lentacker, I., De Cock, I., Deckers, R., De Smedt, S. C., & Moonen, C. T. W. (2014). Understanding ultrasound induced sonoporation: Definitions and underlying mechanisms. *Advanced Drug Delivery Reviews*, *72*, 49-64. https://doi.org/10.1016/j.addr.2013.11.008

Leow, R. S., Wan, J. M., & Yu, A. C. (2015). Membrane blebbing as a recovery manoeuvre in site-specific sonoporation mediated by targeted microbubbles. *Journal of the Royal Society Interface*, *12*(105), 20150029. https://doi.org/10.1098/rsif.2015.0029

Miller, D. L., Pislaru, S. V., & Greenleaf, J. F. (2002). Sonoporation: Mechanical DNA delivery by ultrasonic cavitation. *Somatic Cell and Molecular Genetics*, *27*(1-6), 115-134. https://doi.org/10.1023/A:1022983907223

Qin, P., Xu, L., Han, T., Du, L., & Alfred, C. H. (2016). Effect of non-acoustic parameters on heterogeneous sonoporation mediated by single pulse ultrasound and microbubbles. *Ultrasonics Sonochemistry*, *31*, 107-115. https://doi.org/10.1016/j.ultsonch.2015.12.001

Qiu, Y., Luo, Y., Zhang, Y., Cui, W., Zhang, D., Wu, J., ... & Tu, J. (2010). The correlation between acoustic cavitation and sonoporation involved in ultrasound mediated DNA transfection with polyethylenimine (PEI) in vitro. *Journal of Controlled Release*, *145*(1), 40-48. https://doi.org/10.1016/j.jconrel.2010.04.010

Ross, J. P., Cai, X., Chiu, J. F., Yang, J., & Wu, J. (2002). Optical and atomic force microscopic studies on sonoporation. *The Journal of the Acoustical Society of America*, *111*(3), 1161-1164. https://doi.org/10.1121/1.1448340

Ter Haar, G. (2007). Therapeutic applications of ultrasound. *Progress in Biophysics and Molecular Biology*, *93*(1-3), 111-129. https://doi.org/10.1016/j.pbiomolbio.2006.07.00

Tomizawa, M., Shinozaki, F., Motoyoshi, Y., Sugiyama, T., Yamamoto, S., & Sueishi, M. (2013). Sonoporation: Gene transfer using ultrasound. *World Journal of Methodology*, *3*(4), 39. https://doi.org/10.5662/wjm.v3.i4.39

Van Wamel, A., Kooiman, K., Emmer, M., Ten Cate, F. J., Versluis, M., & de Jong, N. (2006). Ultrasound microbubble induced endothelial cell permeability. *Journal of Controlled Release*, *116*(2), e100-e102. https://doi.org/10.1016/j.jconrel.2006.09.071

Wu, S., Sun, M., Zhang, X., Liao, J., Liu, M., Qin, Q., & Wei, J. (2021). Grouper TRAF4, a novel, CP-interacting protein that promotes red-spotted grouper nervous necrosis virus replication. *International Journal of Molecular Sciences*, *22*(11), 6136. https://doi.org/10.3390/ijms22116136

Yang, Y., Li, Q., Guo, X., Tu, J., & Zhang, D. (2020). Mechanisms underlying sonoporation: Interaction between microbubbles and cells. *Ultrasonics Sonochemistry*, *67*, 105096. https://doi.org/10.1016/j.ultsonch.2020.105096

Zhong, W., Sit, W. H., Wan, J. M., & Alfred, C. H. (2011). Sonoporation induces apoptosis and cell cycle arrest in human promyelocytic leukemia cells. *Ultrasound in Medicine & Biology*, *37*(12), 2149-2159. https://doi.org/10.1016/j.ultrasmedbio.2011.09.012